Discover Environment

Research

Multi-decade land cover/land use dynamics and future predictions for Zambia: 2000–2030

Charles Bwalya Chisanga[1] · **Darius Phiri**[1] · **Kabwe Harnadih Mubanga**[2]

Received: 28 November 2023 / Accepted: 12 April 2024
Published online: 20 April 2024

Abstract
Human LULCC is the many driver of environmental changes. Accurate and up-to-date current and predicted information on LULCC is important in land use planning and natural resource management; however, in Zambia, detailed information on LULCC is insufficient. Therefore, this study assessed the dynamics of LULC change (2000–2020) and future projections (2020–2030) for Zambia. The ESA CCI land cover maps, which have been developed from Sentinel-2 images were used in this study. This dataset has a grid spatial resolution of 300 m for the 2000, 2010 and 2020. The 31 ESA CCI Classification were reclassified into ten (10) local Classifications using the *r.class* module in QGIS 2.18.14. The 2000 and 2010 LULC maps were used to simulate the 2020 LULC scenario using Artificial Neural Network (Multi-layer Perception) algorithms in Modules for Land Use Change Evaluation (MOLUSCE) plugin in QGIS 2.18.14. The 2010 and 2020 maps were used to predict the 2030 LULC classes. The reference 2020 and predicted 2020 LULC maps were used to validate the model. Predicted against observed 2020 LULC map, Kappa (loc) statistic was 0.9869. The 2020 LULC patterns was successfully simulated using ANN-MLP with accuracy level of 95%. LULC classes were predicted for 2030 using the 2010–2020 calibration period. The predicted 2030 LULC types shows an increase in built-up (71.44%) and decrease in cropland (0.73%) with reference to 2020 LULC map. Dense forest (0.19%), grassland (0.85%) and bare land (1.37%) will reduce from 2020–2030. However, seasonally flooded, sparse forest, shrub land, wetland and water body will increase marginally. The largest LULC change is from forest into other LULC types. The insights from this study show that ANN-MLP can be used to predict LULCC, and that the generated information can be employed in land use planning and National Adaptation Plans at regional and national scale.

Keywords Artificial neural network · Cellular automata · European space agency · Land use and land cover change · Multi-layer perceptron

1 Introduction

Land use/land cover change (LULCC) is a significance cause of global environmental change [1, 2]. Land cover is described as the physical and environmental characteristics of the land surface area [3], while land use is the human modification of the surface of the earth [4]. Information on LULCC is key to environmentalists and planners due to its impact on the global environment [5]. The generation of LULCC maps is important in land use planning and natural resources management for the benefit of human needs. The main drivers of regional land cover changes (LCC) are urbanization, deforestation, expansion of agricultural land and alteration of grassland areas [6–8]. In developing countries, urbanization and

✉ Charles Bwalya Chisanga, cbchisanga@gmail.com | [1]School of Natural Resources, Copperbelt University, PES, P. O. Box 21692, Kitwe, Zambia. [2]Geography and Environmental Studies Department, The University of Zambia, Lusaka, Zambia.

agricultural expansion have led to rapid changes in LULC [6, 9].The major drivers of deforestation and forest degradation in developing countries like Zambia include economic development, population growth and lack of good government policies due to limited per capita land and poor adaptability [6, 9–11]. Owing to different factors driving the changes, LULCC occur at different rates and spatio-temporal scale [12, 13].

Geospatial technology, Remote sensing and Geographical Information System (GIS), is increasingly used to monitor the Earth's surface at low costs and within the shortest period of time [14, 15]. The integration of satellite remotely sensed data and GIS is recognized as an effective approach for monitoring and managing natural resources and land use planning [2]. In addition, the advancement in computing technology couples with free access policies on datasets have made it possible to monitor changes at large spatial scales [16, 17]. The study of LULCC detection is important to urban planners, policy makers, natural resource managers, agriculture experts and environmentalist [6, 18, 19].

Different algorithms have been used to predict and simulate the changes in LULC [20–22]. These include Cellular Automata (CA) model namely; Traditional CA (TCA) model, Agents based Cellular Automata (ACA) Model and Neural Network coupled Agents-based Cellular Automata (NNACA) model [19, 23], machine-learning [19, 24], cellular automata-Markov model [5, 25] and Markov chain (MC) [26–29]. The Markov-CA approach has been applied in generating dynamics of LULCC modeling at watershed level in Indonesia [25]. Further, Markov-CA approach has been used to predict future changes in LULC types [29, 30]. The Cellular Automata (CA) model has been used in simulating the spatial LULCC by estimating the state of a pixel according to its initial state, surrounding neighbourhood effects and transition rules [19, 31]. Yang et al. [32] argues that CA models are able to predict the spatial distribution of landscape patterns but fail to predict temporal changes [5, 32]. A combination of CA and ANNs have been used to model LULC dynamics [19, 32, 33]. Other researchers [19, 34] have highlighted that the CA model can generate patterns and effectively represent nonlinear spatial LULCC processes. The CA model has been applied in urban and forest studies [19], and have the capacity to simulate the spatial and temporal complexity of urban areas. Further, forests have also been simulated under the influence of anthropogenic activities and natural hazards [19]. The artificial neural network-based Markov chain model has been applied in simulating LULCCs [35].

Artificial neural network (ANN) is a popular tool used in the analysis of satellite remotely sensed data [15] mainly due to the fact that it characterizes a comparatively new approach to developing predictive models [36]. ANN-MLP has been applied in spatio-temporal modeling of soil erosion studies [37]. In the medical field, this approach has been used to simulate biological nervous systems [38, 39]. The ANN models are being used in the urban spatial growth [40], LULC classification, LULCC detection and LULC prediction since the 1990s [38]. ANN have been integrated with GIS and CA models for predicting LULC [19, 23, 41]. The Artificial Neural Network based Cellular Automaton (ANN-CA) simulate multiple LULCC and complex land use systems [19, 42]. The ANN-CA can be used to determine LULCC by incorporating spatial variables such as slope, aspect and elevation which may influence the changes [19, 42]. An important class of ANN which has been applied and used in many fields is the multilayer perceptron (MLP) [15, 43].

Predicting LULCC is significant for a number of developmental issues including urban expansion, deforestation and forest degradation [42]. Change detection and predicting future LULC categories can provide patterns of future land development based on current and historical changes. The historical changes can be used to identify future problems and uncertainties associated with LULCC. The LULC prediction maps provide vital information concerning types, direction, location and the magnitude of change. The predicted LULC maps can be used to inform policy, assess the developmental impacts and contribute to land use plans. It has been documented that the ESA CCI LULC maps for 2000, 2005, 2010 and 2015 were reasonably accurate at the global level [44, 45]. Furthermore, researchers observed a 60% agreement between the ESA CCI LULC maps and GLC2000, and GLOBCOVER [44, 46, 47].

Researchers such as Guidigan et al. [2] have applied ESA CCI-LC products (2001, 2008, 2013) in Benin. This researcher used QGIS MOLUSCE plugin to validate the model and predict LULC scenarios for 2025 and 2037 and the results indicated an increase in cropland, forest and a reduction in Savannah land. Further, the ESA CCI product is increasingly being applied [48, 49]. However, the paucity information exists on the application of ESA CCI LULC maps over Zambia. In addition, the maps have not been applied in Zambia to predicted future changes in LULC types or impacts of LULCC on the climate. However, they have been applied in Europe to assess the impacts of LULCC on climate [48]. On the other hand, the correlation between ESA CCI LULC maps with independent reference LULC maps for Africa on a continental or regional scale is lacking. Therefore, the objectives of this study were to assess the dynamics of LULCC and to predict 2030 future LULC scenario in Zambia. The insights from this study can be used in sustainable natural resources management and land use planning at a national scale. Further, the results may be used to inform policy and the National Development and Adaptation Plans to formulate strategies to reduce impacts of climate change.

2 Materials and methods

2.1 Description of the study site

Zambia is a landlocked country located in Southern Africa and shares its borders with eight neighboring countries. Tanzania and the Democratic Republic of Congo (DRC) are in the north; Angola in the west; Namibia, Botswana and Zimbabwe in the south, and Mozambique and Malawi in the east (Fig. 1:). It lies between latitudes 7° and 19° South of the Equator and longitudes 21° and 35° East of the Greenwich Meridian. Zambia has a total land surface area of 752,616 km^2 and its altitude range between 1,000 and 1,600 m above sea level [50]. Zambia had an estimated population of 10415944, 13605984, and 18383955 according to World Population Prospects (WPP) of the United Nations, Department of Economic and Social Affairs in 2000, 2010 and 2020, respectively (https://www.worldometers.info/world-population/zambia-population/). By 2030, the population is projected to be 24,325,505 [51].

2.2 Agro-ecological regions and climate

Zambia is divided into three agro-ecological regions (AERs; I, IIA, IIB and III) based on the amount of rainfall, soils properties and other climatic characteristics [52–54] as shown in Fig. 1. AER I, AER II, and AER III receive approximately < 800, 800–1000 and 1000–1500 mm of precipitation per year, respectively. The average annual temperature and rainfall in the AERs varies mostly by elevation [55]. The country is characterized by tropical climate with three distinguishable seasons: hot and dry season from mid-August to November, warm and wet (mid-November to April) and cool and dry (May to mid-August) [56]. The cold temperature ranges from 3.6 °C to 12.0 °C with an average of 8.1 °C, mean hot temperature is 31.8 °C ranging from 27.7 °C to 36.5 °C [57]. The hot summer months are very dry, receiving almost no rainfall between June and August.

Rainfall is extremely variable from year to year with an annual mean rainfall between 600 mm in the southern and 1400 mm in the northern part of Zambia [58]. The annual rainfall is strongly influenced by the shifting of the Pacific Ocean's El Nino Southern Oscillation (ENSO), the Inter-Tropical Convergence Zone (ITCZ) and the Congo Air Boundary and these produces stable rainfall patterns in the northern part of Zambia [55, 59, 60]. The oscillating of the ITCZ between the northern and southern tropics during the course of the rain season leads to downward gradient of rainfall distribution from the north to the south of the country [61]. Multi-decadal trends in these phenomena contribute to annual variations in rainfall patterns and temperatures (Fig. 1).

2.3 Topography

Zambia's topographic features are represented by a series of gently undulating and flat plateau with hills and low ranges. Broad shallow depressions can often be found in the plateau forming swamps and flats. The western part of the country is covered with loose sediment delivered by the Zambezi River which forms a wide flat plain. The plateau is abruptly broken by steep linear escarpments running in a North-east-South-west direction along the Luangwa River and Zambezi River in the south-western peripheral area of Zambia. The plateau has an average elevation of 1300 m above sea level varying from a maximum of 2164 m in the east to a minimum of 325 m at the Zambezi River. Most of the country lies between 900 and 1500 m and the main cities are mainly situated on the gentle undulating plateau [50].

Zambia has a diverse topography that includes high plateaus, mountains, and valleys. The topographic features are represented by a series of gently undulating and flat plateau with hills and low ranges. The country's landscape can be divided into three main regions:

The Zambezi River Valley This region is located in the southern part of the country and is characterized by broad valleys and lowlands. The Zambezi River, which forms Zambia's southern border with Zimbabwe, flows through this region and forms the famous Victoria Falls. Broad shallow depressions can often be found in the plateau forming swamps and flats. The western part of the country is covered with loose sediment delivered by the Zambezi River which forms a wide flat plain.

The Central Plateau This region occupies the central part of the country and is dominated by a high plateau that rises between 1,000 and 1,600 m above sea level. The plateau is broken up by numerous hills and valleys and is dotted with large lakes and rivers. The plateau is abruptly broken by steep linear escarpments running in a North-east-South-west direction along the Luangwa River and Zambezi River in the south-western peripheral area of Zambia. The plateau has

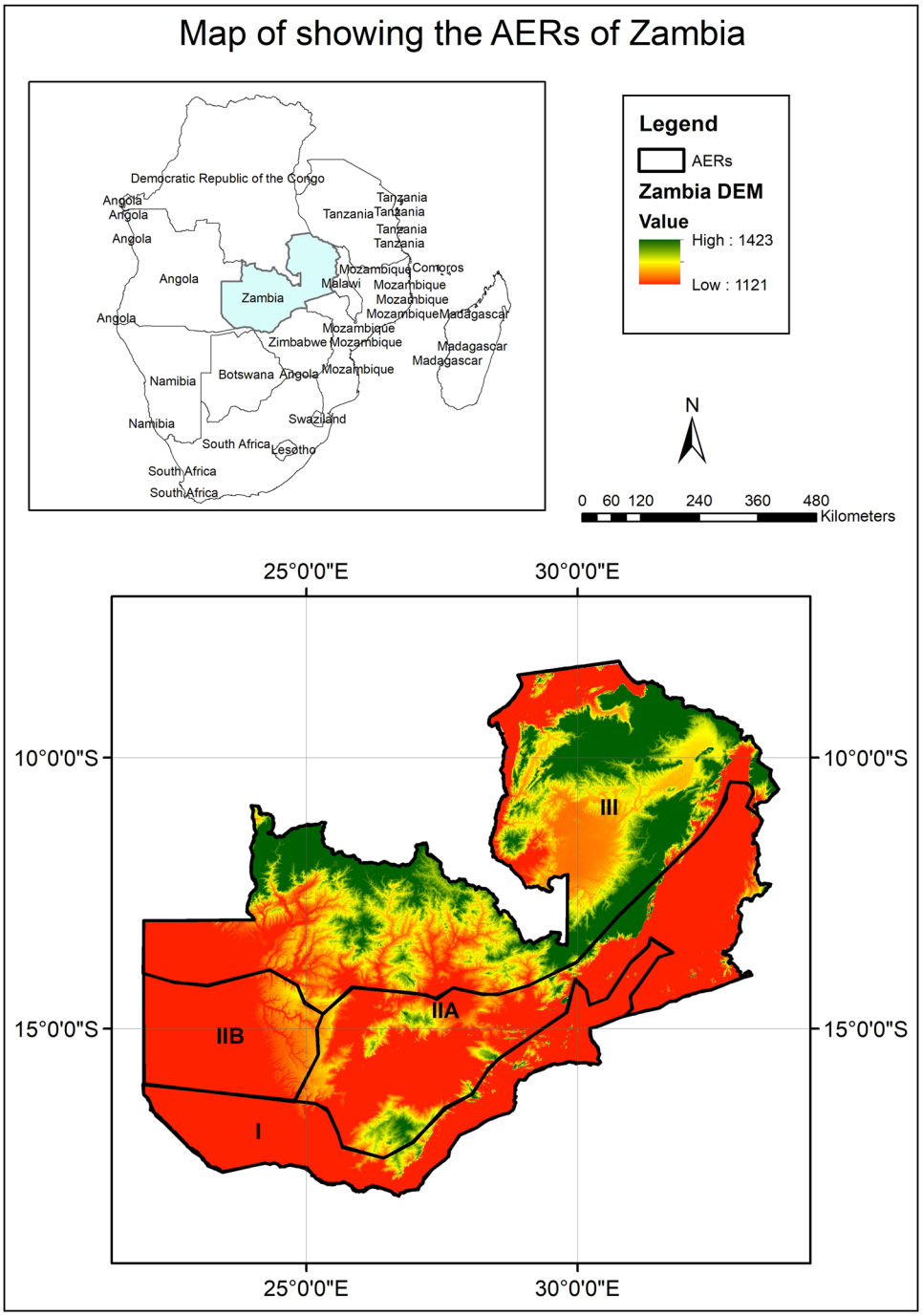

Fig. 1 Map showing the relative position of Zambia with its neighboring countries namely, Tanzania and the Democratic Republic of Congo (DRC), Angola, Namibia, Botswana, Zimbabwe, Mozambique and Malawi

an average elevation of 1300 m above sea level varying from a maxim of 2164 m in the east to a minimum of 325 m at the Zambezi River. The majority of the country lies between 900 and 1500 m and the main cities are mainly situated on the gentle undulating plateau [50].

The Eastern Highlands This region is located in the northeast part of the country and is characterized by high mountains and deep valleys. The highest peak in Zambia, Mount Mafinga, is located in this region and rises to an elevation of 2,339 m above sea level.

2.4 Data source

The European Space Agency (ESA) Climate Change Initiatives (CCI) land cover maps were acquired from Copernicus Climate Data Store (https://cds.climate.copernicus.eu/cdsapp#!/dataset/satellite-land-cover?tab=form) for the year 2000, 2010 and 2020. The land cover maps (LCMs) are provided for versions 2.0.7 (2000 and 2010) and 2.1.1 (2020). The v2.0.7cds provides the LC maps for the years 1992–2015 while v2.1.1 for the years 2016–2019.

The ESA CCI dataset provides global wall-to-wall maps that describe the land surface into 22 classes, which have been defined using the United Nations Food and Agriculture Organization's (UN FAO) Land Cover Classification System (LCCS). In addition to the land cover (LC) maps, four quality flags are produced to document the reliability of the classification and change detection. The ESA CCI land cover maps are consistent with the series of global annual LC maps from the 1990s to 2015 produced by the ESA CCI.

To produce the ESA CCI dataset, the entire Medium Resolution Imaging Spectrometer (MERIS) Full and Reduced Resolution archive from 2003 to 2012 was first classified into a unique 10-year baseline LC map. This is then back- and up-dated using change detected from (i) Advanced Very-High-Resolution Radiometer (AVHRR) time series from 1992 to 1999, (ii) SPOT-Vegetation (SPOT-VGT) time series from 1998 to 2012 and (iii) PROBA-Vegetation (PROBA-V) and Sentinel-3 OLCI (S3 OLCI) time series from 2013 [2, 62]. Beyond the climate-modelling communities, this dataset's long-term consistency, yearly updates, and high thematic detail based on a global scale have made it attractive for a multitude of applications such as land accounting, forest monitoring and desertification, in addition to scientific research [63].

The 2000 and 2010 land use land cover maps were used to simulate the 2020 LULC map using the Modules for Land Use Change Evaluation (MOLUSCE) plugin in QGIS 2.18.14 (https://qgis.org/downloads/). The MOLUSCE is a QGIS plugin for Land Use Change Evaluation. It provides a set of algorithms (Artificial Neural Network-Multi-Layer Perceptron [ANN-MLP], Logistic Regression [LR], Weights of Evidence [WoE], Multi Criteria Evaluation [MCE]) for land use change simulations including kappa statistics for validation [64, 65]. A MLP is an important class of ANN and it has been widely applied in similar studies [15]. MOLUSCE plugin was developed by Asia Air Survey (http://www.asiaairsurvey.com) and NextGIS (http://nextgis.com). Here, the predicted 2020 LULC map was compared with the reference 2020 LULC map to validate the model. Based on the created model, the prediction of future LULC scenario for 2030 was simulated.

2.5 Data processing

The ESA Global land cover datasets for 2000 (C3S-LC-L4-LCCS-Map-300 m-P1Y-2000-v2.0.7cds.tif), 2010 (C3S-LC-L4-LCCS-Map-300 m-P1Y-2000-v2.0.7cds.tif) and 2020 (C3S-LC-L4-LCCS-Map-300 m-P1Y-2020-v2.1.1.tif) were extracted (clip raster by mask layer) using country boundary shapefiles (gadm36zmb0.shp) after being loaded in QGIS. The ESA CCI land cover maps have a grid spatial resolution of 300 m [49, 66]. Additionally, they have a high temporal and spatial consistency and delivers appropriate input for climate modelling [44]. The ESA-CCI LC maps are provided in annual time steps for 1992–2020 [62, 67]. The classification of the LC maps follows the United Nations Land Cover Classification System (UN-LCCS) protocol was used in classifying the ESA CCI LULC maps [67, 68]. They "consists of 22 level 1 classes and 14 additional level 2 classes" [67]. More details on processing ESA-CCI LC datasets is located at maps.elie.ucl.ac.be/CCI/viewer/download/ESACCI-LC-Ph2-PUGv2_2.0.pdf.

The 31 ESA CCI Classification [49] were reclassified into ten (10) local Classifications (Table 1) using the *r.class* module in QGIS 2.18.14. LULCC detection was undertaken on the reclassified LULC maps for 2000, 2010 and 2020. The spatial variables maps included in the analysis were elevation, slope and aspect maps. The aspect and slope maps were generated from the Digital Elevation model (DEM) using QGIS. The final step was to align all LULC maps (2000, 2010, and 2020), elevation and aspect maps. In predicting future changes, we focused on using topographic factors, without including proximity factors as we wanted to understand the influence of topographic factors alone.

The LULCC from 2000–2010, 2010–2020 and 2000–2020 (Fig. 2, Table 4) were analysed using R Programming/RStudio software. The land cover change transition matrix and percentage change in land cover were developed using R/RStudio. The pixel data were resampled from 300 m spatial resolution to a square kilometre.

Table 1 Observed land cover change Matrix between 2000 and 2010

		Year 2010 land cover in km^2										
		1	2	3	4	5	6	7	8	9	10	Sum
Year 2000 land cover in km^2	1	44119.40	0.00	0.00	218.60	116.60	0.00	0.00	7.10	0.00	0.70	44462.40
	2	0.00	15729.20	0.00	222.00	33.90	0.00	0.00	0.00	0.00	0.60	15985.80
	3	0.00	0.00	61960.90	2146.70	261.50	0.70	0.00	14.40	0.00	1.50	64385.70
	4	496.00	161.50	682.40	427629.40	1068.80	68.20	883.60	5.10	7.70	37.00	431039.70
	5	473.70	30.80	543.20	6262.50	119174.50	12.90	6.00	188.10	0.00	28.20	126719.80
	6	8.40	1.00	1.10	27.40	56.40	7947.90	0.00	15.30	0.00	19.00	8076.50
	7	0.00	0.00	0.10	110.00	12.50	0.00	26541.70	0.00	0.00	119.10	26783.40
	8	0.00	0.00	0.00	0.00	0.00	0.00	0.00	391.70	0.00	0.00	391.70
	9	0.40	0.00	0.10	0.00	0.00	0.00	0.00	4.00	36.30	0.00	40.80
	10	0.80	0.00	1.00	5.60	10.40	0.80	81.80	0.20	0.00	13314.10	13414.70
	Sum	45098.60	15922.40	63188.70	436622.20	120734.70	8030.50	27513.20	626.00	43.90	13520.20	731300.50

1 = Cropland; 2 = Seasonally flooded grassland; 3 = Sparse forest; 4 = Dense forest; 5 = Shrub land; 6 = Grassland; 7 = Wetland; 8 = Built-up; 9 = Bare land; 10 = Water body

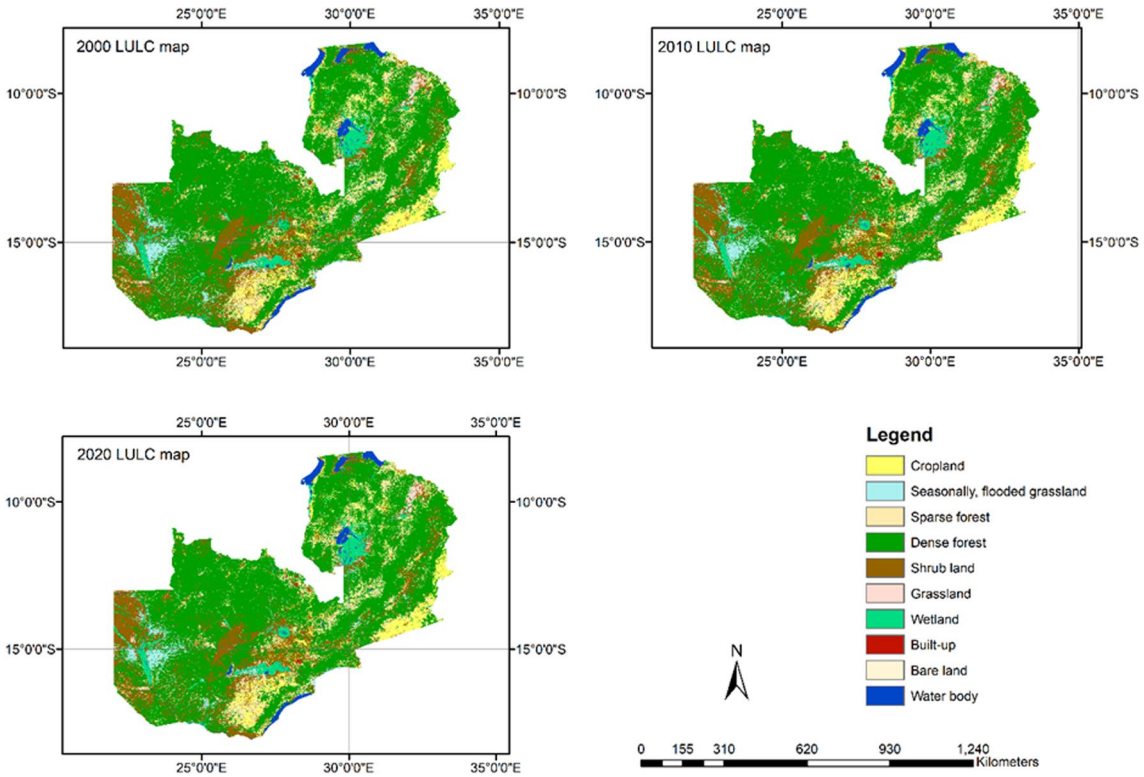

Fig. 2 LULCC maps of Zambia for 2000, 2010 and 2020

2.6 Description of multi-layer perceptron (MLP) model

The MLP is the most popular neural network architecture [69]. ANN-MLP is one of the approaches used with presence/absence data [31]. It is a network of simple neurons called perceptrons. The perceptron computes a single output from multiple real-valued inputs by forming a linear combination according to its input weights and then possibly putting the output through some nonlinear activation function [43]. The MLP is usually trained using the error backpropagation algorithm [70]. The objective of training of an ANN-MLP model is to obtain optimal model

parameters that allow a model to yield the best representation of the input–output relationship of a particular system [43]. The ANN-MLP works by iteratively changing a network's interconnecting weights thus minimizing the overall error between observed and simulated LULC map [71].

2.7 Land use/land cover change prediction and validation

2.7.1 Area changes (change analysis)

The LULCC detection was carried out using land cover maps for 2000, 2010 and 2020. LULCC detection aided in observing the evolution of land class categories during the last twenty years. Area changes were generated from 2000–2010 and 2010–2020. The MOLUSCE plugin allows the generation of class statistics, transition matrix and LULC change map [2]. The class statistics describes changes that have taken place between LULC map at time 0 and time 1 periods. The transition matrix depicts the number of pixels that have changed from one LULC type to another.

2.7.2 Transition potential modelling

The ANN-MLP was selected to perform the transition potential modelling as a pre-stage [2, 72] for prediction 2020 LULC map using the Cellular Automata Simulation based on initial LULCC in 2000 and 2010. The MLP structure consists of three-layer (input, hidden and output layer) [31, 43, 72]. The ANN (MLP) learning process between 2000 and 2010 LULC maps used 1000 iterations, 1-pixel, 0.100 learning rate, 10 hidden layers and 0.050 momentum. The overall accuracy, minimum validation overall error and current validation Kappa were -0.00095, 0.00385 and 0.93984, respectively between the 2000 and 2010 LULC maps.

2.7.3 Cellular automata simulation

The class statistics, transition matrix and LULC change map were used to predict 2020 LULC map using Cellular Automata (CA) Simulation in MOLUSCE plugin. The CA approach is based on Monte Carlo algorithm and every change can be viewed as a transition of land use categories. The change map is a integer one-band raster that stores information about transitions [73]. Furthermore, category values of change map are mapped one-to-one to transition classes. During the second stage, class statistics, transition matrix and LULC change map between 2010 and 2020 LULC map were used to predict the 2030 LULC map using the Cellular Automata Simulation and plausible changes in LULCC determined.

2.7.4 Validation

Ten validation iterations were used to compare the predicted 2020 and observed 2020 LULC map using kappa histogram (khisto), kappa overall (kovr) and kappa location (kloc) [73]. Based on previous studies which were conducted in the same geographic area [74], we used a sample of 1000 points for validation. The MOLUSCE plugin calculates three types of kappa statistic as shown in Eqs. 1, 2 and 3 [19, 75].

$$kappa(K) = \frac{P(A) - P(E)}{1 - P(E)} \tag{1}$$

$$kappalocation\left(K_{loc}\right) = \frac{P(A) - P(E)}{P_{max} - P(E)} \tag{2}$$

$$kappahistogram() = \frac{P_{max} - P(E)}{1 - P(E)} \tag{3}$$

where $P(A) = \sum_{i=1}^{c} P_{ii}$, $P(E) = \sum^{ci=1} P_{iT}P_{Ti}$, $P_{max} = \sum_{i=1}^{c} \min(P_{iT}, P_{Ti})$ and P_{ij} is the i,j-th cell of contingency table, P_{iT} is the sum of all cells in i-th row, P_{Tj} is the sum of all in j-th column, c is the count of raster categories.

3 Results

3.1 multi-temporal changes in LULC from 2000 to 2020

Observed land cover change Matrix between 2000 and 2010, 2010–2020, and 2000–2020 are shown in Tables 1, 2 and 3. The LULCC maps of Zambia for 2000, 2010 and 2020 are shown in Fig. 2. The percentage changes in the ten multi-temporal LULC classes are shown in Table 4. The LULC categories of cropland, seasonally flooded grassland, dense forest, wetland, built-up, bare land and water body increased from 2000 to 2020. Major increase of LULC types from 2000 to 2020 were Built-up (174.01%) followed by Bare land (6.39%). LULC types decreased by 4.58%, 1.42% and 1.22% under Shrub land (5808.50 km^2), Grassland (114.70 km^2) and Sparse forest (788.60 km^2), respectively. During the period 2000 to 2010 and 2010 to 2020, Built-up exhibits a decreasing trend by 59.79% and 71.44%, respectively. Cropland indicated a decrease trend of 0.70%. However, there is an increase of Cropland LULC type from 2000–2010 to 2000–2020 of 1.43% and 0.72%, respectively. The results shows that Built-up area increased while Sparse forest, shrub land and Grassland decreased during the period 2000 to 2020. Moreover, Bare land also increased from 2000 to 2020 by 6.39% (2.60 km^2).

Table 2 Observed land cover change Matrix between 2010 and 2020

		Year 2020 land cover in km^2										
		1	2	3	4	5	6	7	8	9	10	Sum
Year 2010 land cover in km^2	1	44382.20	0.00	0.40	382.00	284.80	0.20	0.00	48.40	0.70	0.10	45098.60
	2	0.00	15738.80	0.00	162.60	19.40	0.20	0.10	1.20	0.00	0.20	15922.40
	3	0.00	0.00	62137.50	864.30	149.00	0.20	0.00	36.90	0.00	0.80	63188.70
	4	300.40	226.20	1275.50	433484.30	1177.40	23.00	89.30	17.50	4.80	24.00	436622.20
	5	87.60	39.50	182.60	869.00	119192.10	11.40	1.20	320.20	0.00	31.10	120734.70
	6	9.10	0.60	0.90	8.10	67.60	7925.40	0.00	17.60	0.00	1.20	8030.50
	7	0.00	0.00	0.10	35.50	11.40	0.00	27385.10	0.20	0.00	80.90	27513.20
	8	0.00	0.00	0.00	0.00	0.00	0.00	0.00	626.00	0.00	0.00	626.00
	9	0.40	0.00	0.00	0.10	0.50	0.00	0.00	5.10	37.80	0.00	43.90
	10	2.70	0.00	0.10	1.70	9.20	1.60	46.60	0.10	0.00	13458.10	13520.20
	Sum	44782.30	16005.10	63597.10	435807.40	120911.50	7961.90	27522.30	1073.20	43.30	13596.50	731300.50

1 = Cropland; 2 = Seasonally flooded grassland; 3 = Sparse forest; 4 = Dense forest; 5 = Shrub land; 6 = Grassland; 7 = Wetland; 8 = Built-up; 9 = Bare land; 10 = Water body

Table 3 Observed land cover change Matrix between 2000 and 2020

		Year 2020 land cover in km^2										
		1	2	3	4	5	6	7	8	9	10	Sum
Year 2000 land cover in km^2	1	43425.50	0.00	0.40	592.20	388.40	0.20	0.00	54.20	0.70	0.80	44462.40
	2	0.00	15551.30	0.00	380.00	51.90	0.30	0.40	1.20	0.00	0.70	15985.80
	3	0.30	0.00	60952.50	2984.20	395.30	0.90	0.30	50.00	0.00	2.30	64385.70
	4	778.50	369.00	1926.90	424644.80	2153.50	90.00	972.60	34.20	11.90	58.30	431039.70
	5	556.30	83.10	714.00	7020.50	117754.60	24.20	9.20	500.10	0.00	57.90	126719.80
	6	17.50	1.60	1.90	35.20	123.50	7844.00	0.10	32.80	0.00	20.10	8076.50
	7	0.00	0.10	0.20	143.40	25.60	0.50	26431.30	0.20	0.00	182.10	26783.40
	8	0.00	0.00	0.00	0.00	0.00	0.00	0.00	391.70	0.00	0.00	391.70
	9	0.70	0.00	0.10	0.10	0.50	0.00	0.00	8.60	30.70	0.00	40.80
	10	3.50	0.00	1.20	7.10	18.10	1.90	108.40	0.30	0.00	13274.30	13414.70
	Sum	44782.30	16005.10	63597.10	435807.40	120911.50	7961.90	27522.30	1073.20	43.30	13596.50	731300.50

1 = Cropland; 2 = Seasonally flooded grassland; 3 = Sparse forest; 4 = Dense forest; 5 = Shrub land; 6 = Grassland; 7 = Wetland; 8 = Built-up; 9 = Bare land; 10 = Water body

Table 4 Land cover change between 2000 and 2010, 2010–2020 and 2000–2020

Classes	2000	2010	2020	2000–2010	% Δ	2010–2020	% Δ	2000–2020	% Δ
Cropland	44462.4	45098.8	44782.4	636.30	1.43	– 316.40	– 0.70	319.90	0.72
Seasonally flooded grassland	15985.7	15922.5	16005.1	– 63.20	– 0.40	82.60	0.52	19.30	0.12
Sparse forest	64385.7	63188.7	63597.1	– 1196.90	– 1.86	408.40	0.65	– 788.60	– 1.22
Dense forest	431039.7	436622.4	435807.6	5582.50	1.30	– 814.80	– 0.19	4767.80	1.11
Shrub land	126719.9	120734.7	120911.4	– 5985.30	– 4.72	176.70	0.15	– 5808.50	– 4.58
Grassland	8076.5	8030.5	7962	– 46.00	– 0.57	– 68.50	– 0.85	– 114.70	– 1.42
Wetland	26783.4	27513.2	27522.3	729.70	2.72	9.10	0.03	738.90	2.76
Built-up	391.7	626	1073.2	234.20	59.79	447.20	71.44	681.60	174.01
Bare land	40.8	43.9	43.3	3.20	7.84	– 0.60	– 1.37	2.60	6.39
Water body	13414.7	13520.1	13596.4	105.50	0.79	76.30	0.56	181.70	1.35

3.2 Validation statistics

The transition potential modelling between 2000 and 2010 LULC map using a random sample of 1000 yielded a current validation kappa of 0.93984. The validation statistics between the predicted 2020 and observed 2020 LULC map indicated that there was a 99.41% of correctness. The kappa (overall), kappa (histo) and kappa (loc) were 0.99122, 0.99754 and 0.9366, respectively. The transition potential modelling between 2010 and 2020 LULC map using a random sample of 1000 yielded a current validation kappa of 0.93128 (Fig. 3).

3.3 Future land use land cover change

The modelled land cover change matrices between 2020 and 2030 are shown in Table 5. Further, Predicted LULCC maps of Zambia for 2030 based on ANN (Multi-layer Perception) are shown in Fig. 4. The predicted maps for 2020 and

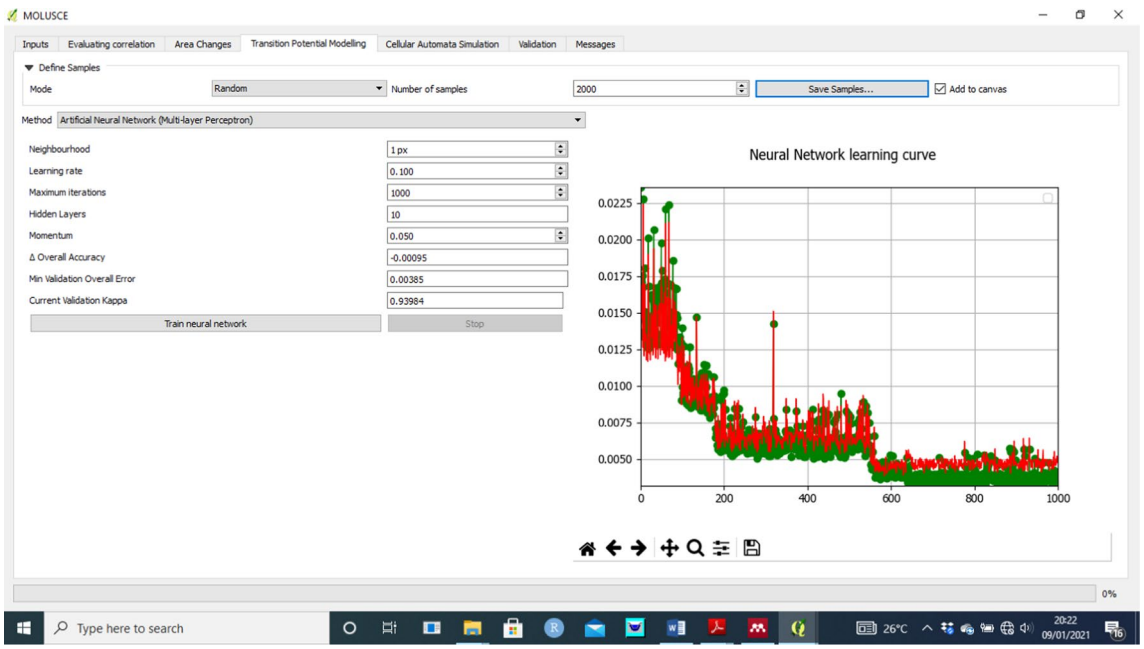

Fig. 3 Transitional potential modelling

Table 5 Predicted land cover change between 2020 and 2030

Classes	2020	2030	2020–2030	% Δ
Cropland	45110.10	44782.30	– 327.80	– 0.73
Seasonally flooded grassland	15911.50	16005.00	93.50	0.59
Sparse forest	63187.70	63597.10	409.40	0.65
Dense forest	436622.40	435807.50	– 814.90	– 0.19
Shrub land	120734.70	120911.40	176.70	0.15
Grassland	8030.50	7962.00	– 68.50	– 0.85
Wetland	27513.60	27522.30	8.70	0.03
Built-up	626.00	1073.20	447.20	71.44
Bare land	43.90	43.30	– 0.60	– 1.37
Water body	13520.10	13596.40	76.30	0.56

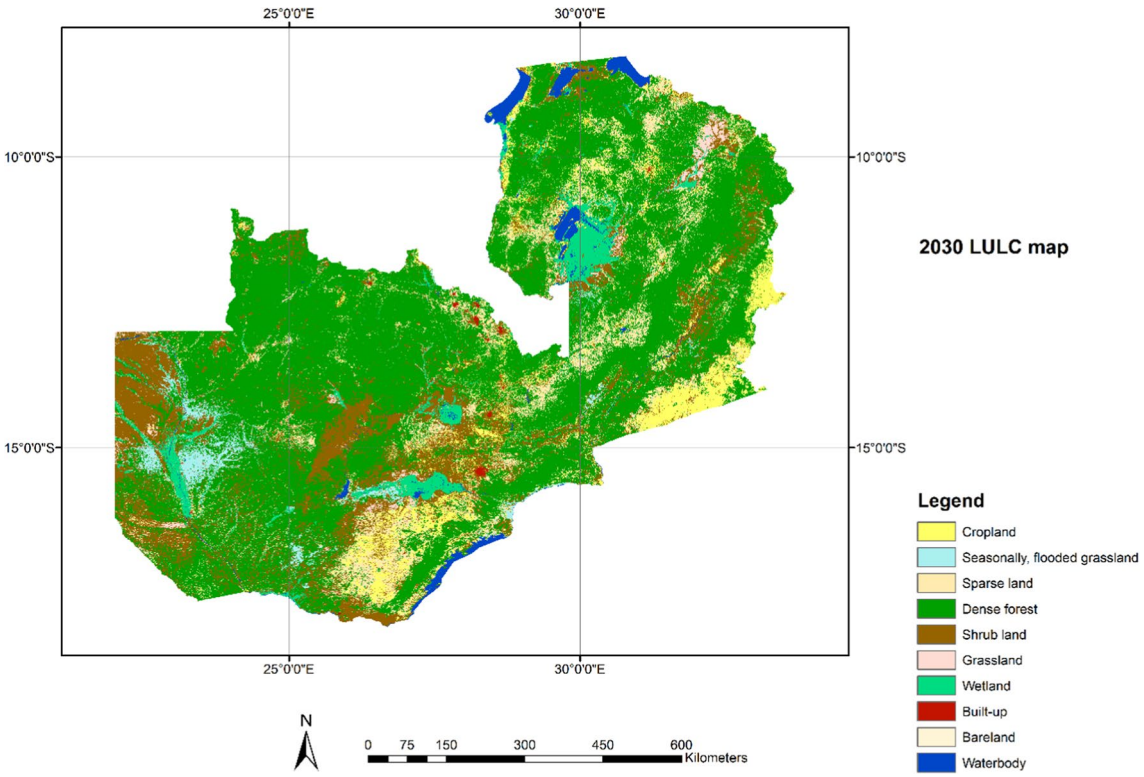

Fig. 4 Predicted LULCC maps of Zambia for 2030 based on ANN (Multi-layer Perception)

2030 LCMs indicates that cropland, dense forest, grassland and bare land categories will reduce by 327.80, 814.90, 68.50 and 0.60 km^2. However, built-up will increase by 71.44% during the same period.

4 Discussions

4.1 Multi-temporal changes in LULC from 2000 to 2020

The findings from this study show that the increase in bare land is because of the decline in forest area. This trend is of great concern to environmentalists and policy makers even in other countries beyond Zambia [6, 76]. It is clear from this study that land cover classes such as built-up and bare land have increased, while dense forest have decline over this period. Evaluating LULCC assessment has revealed that Zambia has been subjected to four diverse rates of land

degradation during the periods of 2000, 2010 and 2020. This is because of upsurge in built-up from 2000 to 2020 of about 681.60 km^2 (174.01%).

From 2000 to 2020, there was an increase in population with corresponding increase in built-up area [77]. This has been necessitated by population expansion which has increased by over 9 million (2010), 13 million (2010), 18 million (2020) and 19 million (2022) [77–81]. Moreover, as of 2010, the population had been growing at approximately 4.2% $year^{-1}$, with 43% of the population living in urban areas [77]. A high rate of population growth exerts pressure on the land and exacerbates shortfalls in cropland [79, 82]. Population growth and expansion in built-up areas are putting more pressure on terrestrial landscapes to meet socio-economic needs such as food and shelter [8].

Understanding LULC dynamic is vital to sustainable development in Zambia where deforestation is a common problem and a great concern to various stakeholders. The prominent cause of forest loss is the expansion of development projects, including settlements and cropland, into forested area [6]. In east African, cropland expansion has led to losses in forest, wetland and grassland LULC types [83]. Hossain et al. [6] has reported similar results in Bangladesh where Built-up (settlement) expanded due to massive human migration into urban areas. The decline in the area covered by forests affects other sectors such as conservation as these areas are habit of different fauna species – some are facing different threats and might go into extinction.

4.2 Future LULCCs

Results from this study also show that built-up will increase by 71.44% during the projected period. Similar results have been reported by chisanga et al. [30] who noted that built-up area will increase by 2030. Others studies revealed an increase in built-up LULC types [41]. In contrast, other researchers have predicted 2030 LULCs using the 2010–2020 calibration period. The largest changes were associated with conversion of forest lands into other land uses [28].

The United Nations (2014) predicts that the share of global urban population will increase from the current 50% to approximately 70% by 2050 [84]. Alongside with this rapid urbanization of the human society, it is estimated that, by 2030, cities will physically expand by 1.2 million km^2, which is almost same size as the Republic of South Africa [84, 85]. The expansion of built-up area by 2030 may led to degradation of ecosystems in most developing countries [86]. Additionally, anthropogenic LULCC is the many driver of environmental changes [48]. Simulating LULCC provides insights, patterns and identifies human impacts like deforestation and forest degradation. The identified environmental problems can be incorporated in the processes of land use planning. Other researchers have noted that monitoring and LULC modelling is imperative in environmental planning, conservation of natural resources and in attaining Sustainable Development Goals (SDGs) number 13 and 15 [6, 87, 88].

The findings of this study contributes to Zambia's Vision 2030 for sustainable socio-economic development [89]. The population of Zambia is projected to be 24 million by 2030 [51]. Further, the simulated LULC maps can be used to articulate long-term plans national development, and achieving the desirable socio-economic outcomes by 2030. The simulation of LULCC provides an understanding of future LULC scenarios [19]. Simulation of LULCC is important for a variety of planning, monitoring, management and academic research. It provides historical LULCC, and how future LULC classes will change based on the current development processes into the future [42].

Elsewhere, other researchers [2, 9, 19, 41, 65, 90–92] have used Open Source Software to analyse and predict future LULCC using tools such as QGIS (*MOLUSCE plugin*) and R Programming packages (*lulcc* R package). Suprayogi and Subiyanto [91] used the *lulcc* package in R/RStudio to model the land use change of Banyumanik. The use of open-source software and open access dataset is a clear testament that monitoring of LULC can be done with less challenges and information can be generated with easy.

4.3 Limitation of the study

The findings of this study need to be interpreted by taking into consideration the research limitations. Firstly, we considered analysis period of 10 years, which is a common practise among researchers; however, some changes might have occurred within this period that went unnoticed. For example, cropland used for less than 5 years and left as fallows and settlements which were abandoned. Secondly, we focused more on topographic factors in predicting our future LULC status without considering other factors such as proximity and socioeconomics. This was done deliberately in order to understand the influence of topographic factors on LULCC in isolation. This approach was ideal for those areas which have limited access and have less socioeconomic activities. Finally, although we achieve high accuracies (> 95%) in our validation, it is still important to note that there is still room for error on our results; however, this is expected to be minimal.

5 Conclusions

This study aimed to understand the multi-decade LULC changes, as well as predicting the future status of land cover for Zambia at a national scale. The growth in built-up and use of ANN-MLP models in LULC prediction could be used for the successful land use planning in forest and natural resource management. The insights from this study are key in conservation, forest monitoring and general LULCC dynamics in order to balance the trade-off between human needs which are driven by population growth on one hand, and conservation needs on the other hand. Being one of the first studies on predicting LULCC for Zambia, the finding from this study will be key in strategic planning for different developmental aspects that concern land at a national scale. Different sectors such forestry, agriculture, and infrastructure can employ these results in their strategic planning and operations.

This study also demonstrates that open access tools and free access datasets can be employed to provide key information on LULC at large scale. The introduction of free access dataset such as Landsat and Sentinel dataset have revolutionised land cover monitoring over the past decades as many resource-constrained scientist have employed these datasets to address different research questions and challenges. As demonstrated in this study, MOLUSCE plugin in QGIS 2.18.14 and R/RStudio can be used to predicted and analyse future LULCC which is important in land use planning including urban planning and in decision making process. Beside the open access tool and free access datasets, the increasing computing capabilities through affordable local computers and cloud computing have also contributed significantly towards LULC monitoring, especially in developing countries such as Zambia. Future studies need to focus on future prediction by using a wide range of factors such as proximity factors (e.g. roads, railway) and socioeconomic factors (e.g., population density, unemployment rate). The study suggests a need to disaggregate the findings at district, provincial and agro-ecological regions which may inform policy, national development plans and National Adaptation Plans (NAPs).

Acknowledgements The authors would want to thank Copernicus for the provision of the LULC maps for 2000, 2010 and 2020. The authors also thanks the QGIS Team for the provision of QGIS 2.18.14 that was used in this study.

Author contributions CBC came up with the concept and wrote the main manuscript text. CBC downloaded the data, reclassified the maps, and conducted the change detection and predictions. Figures and Tables were generated by CBC and DP. DP proofread the manuscript and made the necessary changes. KHM also proofread the manuscript. CBC separated the results and discussion sections. Revisions were made by CBC and DP. DP added more text and explanation to the abstract and conclusion.

Funding There was no funding for this study.

Data availability The datasets analysed during the current study are available on Copernicus Climate Data Store repository (https://cds.climate.copernicus.eu/cdsapp#!/dataset/satellite-land-cover?tab=form). The reclassified datasets are available from the corresponding author on reasonable request.

Declarations

Competing interests The corresponding author states that there is no conflict of interest.

References

1. Song X, Hansen MC, Stehman SV, et al. Global land change 1982–2016. Nature. 2018;560:639–43. https://doi.org/10.1038/s41586-018-0411-9.
2. Guidigan MLG, Sanou CL, Ragatoa DS, et al. Assessing land use/land cover dynamic and its impact in benin republic using land change model and CCI-LC products. Earth Syst Environ. 2019;3:127–37. https://doi.org/10.1007/s41748-018-0083-5.
3. Turner BL. Local faces, global flows: the role of land use and land cover in global environmental change. L Degrad Dev. 1994;5:71–8. https://doi.org/10.1002/ldr.3400050204.
4. Batunacun NC, Hu Y, Lakes T. Land-use change and land degradation on the Mongolian Plateau from 1975 to 2015-A case study from Xilingol, China. L Degrad Dev. 2018;29:1595–606. https://doi.org/10.1002/ldr.2948.

5. Islam K, Rahman MF, Jashimuddin M. Modeling land use change using cellular automata and artificial neural network: the case of Chunati wildlife sanctuary, Bangladesh. Ecol Indic. 2018;88:439–53. https://doi.org/10.1016/j.ecolind.2018.01.047.
6. Hossain MS, Khan MAH, Oluwajuwon TV, et al. Spatiotemporal change detection of land use land cover (LULC) in Fashiakhali wildlife sanctuary (FKWS) impact area, Bangladesh, employing multispectral images and GIS. Model Earth Syst Environ. 2023. https://doi.org/10.1007/s40808-022-01653-7.
7. Lambin EF, Turner BL, Geist HJ, et al. The causes of land-use and land-cover change: moving beyond the myths. Glob Environ Chang. 2001;11:261–9. https://doi.org/10.1016/S0959-3780(01)00007-3.
8. Bowler DE, Bjorkman AD, Dornelas M, et al. Mapping human pressures on biodiversity across the planet uncovers anthropogenic threat complexes. People Nat. 2020;2:380–94. https://doi.org/10.1002/pan3.10071.
9. Ibrahim WYW, Ludin ANM. Spatiotemporal land use change analysis using open-source GIS and web based application. Int J Built Environ Sustain. 2014;2:10. https://doi.org/10.11113/ijbes.v2.n2.64.
10. Fagan ME, Reid JL, Holland MB, et al. How feasible are global forest restoration commitments? Conserv Lett. 2020;13:8. https://doi.org/10.1111/conl.12700.
11. Diouf A, Lambin EF. Monitoring land-cover changes in semi-arid regions: remote sensing data and field observations in the Ferlo, Senegal. J Arid Environ. 2001;48:129–48. https://doi.org/10.1006/jare.2000.0744.
12. DeFries RS, Rudel T, Uriarte M, Hansen M. Deforestation driven by urban population growth and agricultural trade in the twenty-first century. Nat Geosci. 2010;3:178–81. https://doi.org/10.1038/ngeo756.
13. Hansen MC, Potapov PV, Goetz SJ, et al. Mapping tree height distributions in Sub-Saharan Africa using Landsat 7 and 8 data. Remote Sens Environ. 2016;185:221–32. https://doi.org/10.1016/j.rse.2016.02.023.
14. Mas JF, Lemoine-Rodríguez R, González-López R, et al. Land use/land cover change detection combining automatic processing and visual interpretation. Eur J Remote Sens. 2017;50:626–35. https://doi.org/10.1080/22797254.2017.1387505.
15. Mas JF, Flores JJ. The application of artificial neural networks to the analysis of remotely sensed data. Int J Remote Sens. 2008;29:617–63. https://doi.org/10.1080/01431160701352154.
16. Turner W, Rondinini C, Pettorelli N, et al. Free and open-access satellite data are key to biodiversity conservation. Biol Conserv. 2015;182:173–6. https://doi.org/10.1016/j.biocon.2014.11.048.
17. Woodcock CE, Allen R, Anderson M, et al. Free access to landsat imagery. Science. 2008;320:1011. https://doi.org/10.1126/science.320.5879.101.
18. Babalola O, Akinsanola A. Change detection in land surface temperature and land use land cover over Lagos Metropolis, Nigeria. J Remote Sens GIS. 2016;5:1–7. https://doi.org/10.4172/2469-4134.1000171.
19. Saputra MH, Lee HS. Prediction of land use and land cover changes for North Sumatra, Indonesia, using an artificial-neural-network-based cellular automaton. Sustainability. 2019;11:1–16. https://doi.org/10.3390/su11113024.
20. Rahaman MH, Saha TK, Masroor M, et al. Trend analysis and forecasting of meteorological variables in the lower Thoubal river watershed, India using non-parametrical approach and machine learning models. Model Earth Syst Environ. 2023. https://doi.org/10.1007/s40808-023-01799-y.
21. Roushangar K, Alami MT, Golmohammadi H. Modeling the effects of land use/land cover changes on water requirements of Urmia Lake basin using CA-Markov and NETWAT models. Model Earth Syst Environ. 2023;9:2569–81. https://doi.org/10.1007/s40808-022-01635-9.
22. Shahfahad TS, Ghose B, et al. Predicting long term regional drought pattern in Northeast India using advanced statistical technique and wavelet-machine learning approach. Model Earth Syst Environ. 2023. https://doi.org/10.1007/s40808-023-01818-y.
23. Devendran AA, Lakshmanan G. The Egyptian journal of remote sensing and space sciences urban growth prediction using neural network coupled agents-based Cellular Automata model for Sriperumbudur Taluk, Tamil Nadu, India. Egypt J Remote Sens Sp Sci. 2018;21:353–62. https://doi.org/10.1016/j.ejrs.2017.12.004.
24. Elmes A, Alemohammad H, Avery R, et al. Accounting for training data error in machine learning applied to earth observations. Remote Sens. 2020;12:1–39. https://doi.org/10.3390/rs12061034.
25. Yulianto F, Prasasti I, Pasaribu JM, et al. The dynamics of land use/land cover change modeling and their implication for the flood damage assessment in the Tondano watershed, North Sulawesi. Indonesia Model Earth Syst Environ. 2016;2:20. https://doi.org/10.1007/s40808-016-0100-3.
26. e Silva LP, Xavier AP, da Silva RM, Santos CA. Modeling land cover change based on an artificial neural network for a semiarid river basin in northeastern Brazil. Glob Ecol Conserv. 2020;21:18. https://doi.org/10.1016/j.gecco.2019.e00811.
27. Anand J, Gosain AK, Khosa R. Prediction of land use changes based on land change modeler and attribution of changes in the water balance of Ganga basin to land use change using the SWAT model. Sci Total Environ. 2018;644:503e519. https://doi.org/10.1016/j.scitotenv.2018.07.017.
28. Shahi E, Karimi S, Jafari HR. Monitoring and modeling land use/cover changes in Arasbaran protected area using and integrated Markov chain and artificial neural network. Model Earth Syst Environ. 2020;6:1901–11. https://doi.org/10.1007/s40808-020-00801-1.
29. Allahyari H, Salehi E. Presentation of a suitable approach for green programming of urban ways through integrative method CA-Markov: case study—Azadi Street of Tehran. Iran Model Earth Syst Environ. 2020;6:373–82. https://doi.org/10.1007/s40808-019-00685-w.
30. Chisanga CB, Shepande C, Nkonde E. CA-Markov Approach in Dynamic Modelling of LULCC Using ESA CCI Products Over Zambia. In: Geographic Information System [Working Title]. IntechOpen, 2022; p 17.
31. Eastman RJ. TerrSet geospatial monitoring and modeling system—manual. Clark Labs: Clark University, Worcester, USA; 2016.
32. Yang C, Wu G, Chen J, et al. Simulating and forecasting spatio-temporal characteristic of land-use/cover change with numerical model and remote sensing: a case study in Fuxian Lake Basin, China. Eur J Remote Sens. 2019;52:374–84. https://doi.org/10.1080/22797254.2019.1611387.
33. Eastman JR. IDRISI Taiga: Guide to GIS and image processing volume—manual version 16.02. Clark Labs, Clark University, Worcester, MA, USA. 2009.
34. Liu X, Liang X, Li X, et al. A future land use simulation model (FLUS) for simulating multiple land use scenarios by coupling human and natural effects. Landsc Urban Plan. 2017;168:94–116. https://doi.org/10.1016/J.LANDURBPLAN.2017.09.019.

35. Debnath M, Islam N, Gayen SK, et al. Prediction of spatio-temporal (2030 and 2050) land-use and land-cover changes in Koch Bihar urban agglomeration (West Bengal), India, using artificial neural network-based Markov chain model. Model Earth Syst Environ. 2023. https://doi.org/10.1007/s40808-023-01713-6.
36. Blackard JA, Dean DJ. Comparative accuracies of artificial neural networks and discriminant analysis in predicting forest cover types from cartographic variables. Comput Electron Agric. 1999;24:131–51. https://doi.org/10.1016/S0168-1699(99)00046-0.
37. Cherif K, Yahia N, Bilal B, Bilal B. Erosion potential model-based ANN-MLP for the spatiotemporal modeling of soil erosion in wadi Saida watershed. Model Earth Syst Environ. 2023. https://doi.org/10.1007/s40808-022-01657-3.
38. Gopal S. Artificial neural networks in geospatial analysis. Int. Encycl. Geogr. 2017; 1–7.
39. Talukdar S, Singha P, Shahfahad SM, et al. Land-use land-cover classification by machine learning classifiers for satellite observations-A review. Remote Sens. 2020;12:24. https://doi.org/10.3390/rs12071135.
40. Kumar M, Kumar V, Rajagopal BG, et al. State of art soft computing based simulation models for bearing capacity of pile foundation: a comparative study of hybrid ANNs and conventional models. Model Earth Syst Environ. 2022;9:1–19. https://doi.org/10.1007/s40808-022-01637-7.
41. Buğday E, Erkan Buğday S. Modeling and simulating land use/cover change using artificial neural network from remotely sensing data. Cerne. 2019;25:246–54. https://doi.org/10.1590/01047760201925022634.
42. Li X, Yeh AGO. Neural-network-based cellular automata for simulating multiple land use changes using GIS. Int J Geogr Inf Sci. 2002;16:323–43. https://doi.org/10.1080/13658810210137004.
43. Oyebode O, Stretch D. Neural network modeling of hydrologicalsystems: a review of implementation techniques. Nat Resour Model. 2019;32: e12189. https://doi.org/10.1002/nrm.12189.
44. Reinhart V, Fonte CC, Hoffmann P, et al. Comparison of ESA climate change initiative land cover to CORINE land cover over Eastern Europe and the Baltic States from a regional climate modeling perspective. Int J Appl Earth Obs Geoinf. 2021;94:12. https://doi.org/10.1016/j.jag.2020.102221.
45. Achard F, Bontemps S, Lamarche C, et al. Quality assessment of the CCI land cover maps. 2017.
46. Koubodana DH, Diekkrüger B, Näschen K, et al. Impact of the accuracy of land cover data sets on the accuracy of land cover change scenarios in the Mono River Basin, Togo, West Africa. Int J Adv Res. 2019. https://doi.org/10.23953/cloud.ijarsg.422.
47. Hua T, Zhao W, Liu Y, et al. Spatial consistency assessments for global land-cover datasets: a comparison among GLC2000, CCI LC, MCD12, GLOBCOVER and GLCNMO. Remote Sens. 2018;10(11):1846.
48. Hoffmann P, Reinhart V, Rechid D, et al. High-resolution land use and land cover dataset for regional climate modelling: a plant functional type map for Europe 2015. Earth Syst Sci Data. 2023;15:3819–52. https://doi.org/10.5194/essd-14-1735-2022.
49. European Space Agency. Land cover CCI product user guide version 2. Tech. Rep. ESA CCI partnership, UCL-Geomatics, Belgium. 2017.
50. Chigunta F, Matshalaga N. Evaluation of the implementation of the Paris declaration in Zambia. Lusaka, Zambia. 2010.
51. UNDESA. World population prospects 2019: Data Booklet (ST/ESA/SER.A/424). 2019; 28.
52. Mubanga KH, Chisanga CB, Chirwa MS, et al. Climate change impacts and adaptation measures. In: third national communication to the united nations framework convention on climate change (UNFCCC). Government Printers, Lusaka, Zambia, 2020; pp 77–96
53. Bailey M, Heinrich D, Kruczkiewicz A. Climate Profiles of Countries in Southern Africa: Zambia. 2021; 5.
54. Suman J. An empirical economic assessment of impacts of climate change on agriculture in Zambia. 2007.
55. USAID. Zambia environmental threats and opportunities assessment (ETOA). 2011.
56. NAPA. Formulation of the national adaptation programme of action on climate change (Final Report). Lusaka, Zambia: Ministry of Tourism, environmentt and natural resources. 2007.
57. Kasali G. Capacity strengthening in the least developed countries(LDCs) for adaptation to climate change (CLACC): Climate change and health in Zambia. Internation institute for environment and development. 2008.
58. GIZ. Integrating Climate Change into Financial Planning: Climate Proofing Manual for Zambia. 2014.
59. MTENR. National climate change response strategy (NCCRS) ministry of tourism, environment and natural resources. Lusaka, Zambia: Government of the Republic of Zambia; 2010.
60. MTENR, GEF, UNDP. Formulation of the national adaptation programme of action on climate change. Ministry of Tourism, Environmental and Natural Resources, Lusaka, Zambia. 2007.
61. Libanda B, David A, Banda N, et al. Predictor selection associated with statistical downscaling of precipitation over Zambia. Asian J Phys Chem Sci. 2016;1:1–9. https://doi.org/10.9734/AJOPACS/2016/31545.
62. ESA. Land Cover CCI product user guide version 2.0. 105. 2017.
63. ESA. ESA Quick user guide of the Land Cover State products in GTiff and NetCDF formats. 2015; 2.
64. Alam N, Saha S, Gupta S, Chakraborty S. Prediction modelling of riverine landscape dynamics in the context of sustainable management of floodplain: a geospatial approach. Ann GIS. 2021;27:299–314. https://doi.org/10.1080/19475683.2020.1870558.
65. Hakim AMY, Baja S, Rampisela DA, Arif S. Spatial dynamic prediction of landuse/landcover change (case study: Tamalanrea sub-district, makassar city). In: The 4th International Conference of Indonesian Society for Remote Sensing. IOP Conference Series: Earth and Environmental Science. 2019; p 8.
66. ESA. Climate Change Initiative: land cover Newsletter. Newsletter;2017; 1–4
67. Reinhart V, Hoffmann P, Rechid D, Bechtel B. High-resolution land-use land-cover change data for regional climate simulations over Europe—part I: the plant functional type basemap for 2015. 2021. Earth Syst Sci Data. https://doi.org/10.5194/essd-2021-251.
68. Di Gregorio A. Land cover classification system: classification concepts and user manual: LCCS. 2005; 2.
69. Mutlu E, Chaubey I, Hexmoor H, Bajwa SG. Comparison of artificial neural network models for hydrologic predictions at multiple gauging stations in an agricultural watershed. Hydrol Process. 2008. https://doi.org/10.1002/hyp.7136.
70. Cao M, Zhu Y, Quan J, et al. Spatial sequential modeling and predication of global land use and land cover changes by integrating a global change assessment model and cellular automata. Earth's Futur. 2019;7:1102–16. https://doi.org/10.1029/2019EF001228.
71. Sudheer KP. Modeling hydrological processes using neural computing technique. Indian Institute of Technology, Delhi, India. 2000.
72. Mangel N, Berhe F. Dynamic land use change prediction and analysis of its impacts on streamflow for Dabus Watershed, Upper Blue Nile Basin. 2021; 1–9.

73. Asia Air Survey and Next GIS. MOLUSCE: modules for land use change evaluation. 2017.
74. Phiri D, Morgenroth J, Xu C. Four decades of land cover and forest connectivity study in Zambia—an object-based image analysis approach. Int J Appl Earth Obs Geoinf. 2019;79:97–109. https://doi.org/10.1016/j.jag.2019.03.001.
75. Pontius RG Jr. Quantification error versus location error in comparison of categorical maps. Photogramm Eng Remote Sensing. 2000;66:1011–6.
76. Oluwajuwon TV, Alo AA, Ogana FN, Adekugbe OA. Forest Cover Dynamics of a lowland rainforest in Southwestern Nigeria using GIS and remote sensing techniques. J Geogr Inf Syst. 2021;13:83–97. https://doi.org/10.4236/jgis.2021.132006.
77. CSO. 2010 Census of population and housing. Population summary report. Lusaka, Zambia. 2012.
78. Moyo N, Nanyangwe-Moyo T, Mapoma CC, et al. The population of the himalayan region: past, present, and future. Res Sq 1–24. 2022.
79. Population Reference Bureau. Managing our population for a healther and more prosperous Zambia. 2019l; 4.
80. ZamStat. 2022 Census of population and housing. Preliminary report. Lusaka, Zambia. 2022.
81. CSO. Summary report for the 2000 census of population and housing. Lusaka, Zambia. 2003.
82. CSO. 2010 census of population and housing. Lusaka, Zambia 2011.
83. Kipkulei HK, Bellingrath-Kimura SD, Lana M, et al. Modelling cropland expansion and its drivers in Trans Nzoia County, Kenya. Model Earth Syst Environ. 2022;8:5761–78. https://doi.org/10.1007/s40808-022-01475-7.
84. Tateishi E. An Application of NASA MODIS remote sensing images to a comprehensive estimation of ecological impacts of urban development. 2015; 8.
85. Seto KC, Güneralp B, Hutyra LR. Global forecasts of urban expansion to 2030 and direct impacts on biodiversity and carbon pools. In: Proceedings of the National Academy of Sciences of the United States of America. 2012; pp 16083–8
86. Ackom EK, Adjei KA, Odai SN. Monitoring land-use and land-cover changes due to extensive urbanization in the Odaw river basin of Accra, Ghana, 1991–2030. Model Earth Syst Environ. 2020;6:1131–43. https://doi.org/10.1007/s40808-020-00746-5.
87. Redowan M, Akter S, Islam N. Analysis of forest cover change at Khadimnagar national park, Sylhet, Bangladesh, using Landsat TM and GIS data. J For Res. 2014;25:393–400. https://doi.org/10.1007/s11676-014-0467-9.
88. Rawat JS, Kumar M. Monitoring land use/cover change using remote sensing and GIS techniques: a case study of Hawalbagh block, district Almora, Uttarakhand, India. Egypt J Remote Sens Sp Sci. 2015;18:77–84. https://doi.org/10.1016/j.ejrs.2015.02.002.
89. GRZ (2006) Zambia Vision 2030. 42
90. AlgNM A-R. Land use change analysis and modeling using open source (QGIS) case study: Boasher Willayat. Oman: Sultan Qaboos University; 2017.
91. Suprayogi A, Subiyanto S. Object Oriented Land Use Change Modelling Of Residential Areas (Case Study : Banyumanik Sub-District, Semarang City). In: GEODETA 2019: The 1st International Conference on Geodesy, Geomatics, and Land Administration 2019 Volume 2019 Conference. KnE Engineering, 2019; pp 303–312.
92. Moulds S, Buytaert W, Mijic A. An open and extensible framework for spatially explicit land use change modelling in R: the lulccR package (0.1.0). Geosci Model Dev Discuss. 2015;8:3359–402. https://doi.org/10.5194/gmdd-8-3359-2015.